A Percolation View of Novolak Dissolution and Dissolution Inhibition

Tung-Feng Yeh, Hsiao-Yi Shih, and Arnost Reiser*

Institute of Imaging Sciences, Polytechnic University, Brooklyn, New York 11201

Received March 31, 1992

ABSTRACT: The dissolution of novolak and other phenolic resins in aqueous alkali is controlled by the diffusion of developer base through a thin penetration zone which separates the matrix from the developer solution. Diffusion of base through the zone is a percolation process which may be described by a scaling law of the form R = constant × $(p - p_c)^2$. Here R is the dissolution rate, p is a percolation parameter which is proportional to the concentration of phenol groups in the solid resin, and p_c is a percolation threshold below which dissolution does not occur. The scaling law of percolative dissolution was tested and confirmed on a group of partially methylated poly(vinylphenol) resins. Theory predicts a relation between the inhibition effect and the rate of dissolution which may be summarized by the expression $-\mathrm{d} \log R/\mathrm{d}c_i = f_{ij} = \alpha_i \mathrm{d} \log R/\mathrm{d}p = \alpha_i (2 \log e)/(p - p_c)$. This has been confirmed by experiment. The constant α_i is an absolute measure of the inhibition capability of an additive without reference to a specific resin.

Positive resists based on the inhibition of novolak dissolution are presently the most widely used imaging materials of the semiconductor device industry. They were discovered by Suess[1,2] in the 1940s at Kalle AG, Wiesbaden, Germany, following the observation that films of pure novolak dissolved in aqueous alkali within minutes, while similar films containing a diazoquinone derivative took an hour or more to dissolve. Evidently, diazoquinone inhibited the dissolution of novolak. Resists based on novolak have now been used for almost 50 years, yet dissolution inhibition is still not properly understood.

The key to an understanding of the molecular mechanism of novolak dissolution and dissolution inhibition is the recognition that novolak and other phenolic resins are amphiphilic materials which contain hydrophilic as well as hydrophobic moieties. A solid novolak film may in effect be regarded as a hydrophobic continuum in which hydrophilic ionizable sites are embedded. On immersion of the film in aqueous alkali, base enters the solid at hydrophilic surface sites and turns some of the phenols into phenolates, or more accurately into phenolate–cation pairs. When the solubility of phenolate in the resin is exceeded, a new phase is formed, a thin subsurface layer separating the developer solution from the solid polymer. This new phase is termed the penetration zone.[3,4] In the stationary state of the dissolution process the rate of dissolution of the resin is controlled by the diffusion of base through the penetration zone.[5]

The diffusion of base into novolak differs from the diffusion of solvent into common polymers in one important respect: in novolak the diffusant is repelled by one of the components of the system, namely, the hydrophobic body of the resin, and it is attracted to the other, i.e., to the hydrophilic phenols and phenolates. As a result, base does not diffuse uniformly through the volume of the polymer but progresses by a series of jumps or transfers from one hydrophilic site to the next.

The progress of a mobile entity through an ensemble of sites, to some of which it is attracted while it has to avoid others, occurs in a variety of situations, e.g., in the propagation of forest fires in sparse tree growth. The statistics of such systems constitute what is known as percolation theory. This paper attempts to develop a model of novolak dissolution and dissolution inhibition on the basis of percolation theory.

Percolation Theory

Percolation theory[6,7] describes diffusion as the progression of a mobile particle through a system of cells, some of which are "occupied" and others empty. The particle is allowed to reside only in occupied cells and may transfer from one occupied cell to its occupied neighbor, but it cannot reach a non-nearest neighbor directly. As a result, the movement of the particle is circumscribed by the size of the cluster of the occupied cells in which it happens to be located. Figure 1 is a schematic representation of a percolation field where only the occupied cells are indicated by open circles.

The overall state of the percolation field is characterized by a parameter p which represents the degree of occupation of the cells. As p increases, so does the average size of the cell clusters and so does the range of migration of the mobile particle. Continuous diffusion throughout the percolation field becomes possible when at least one "infinite" cluster has formed, i.e., a cluster which extends through the whole width of the field. The p value at which the first infinite cluster appears is called the (critical) percolation threshold, p_c, of the system.

It is a fundamental thesis of percolation theory that the macroscopic properties of percolation systems are unique functions of the difference $(p - p_c)$. For percolative diffusion this function has the form of a scaling law.

$$D = \text{constant} \times (p - p_c)^n \qquad (1)$$

Novolak dissolution corresponds to base diffusion through a three-dimensional system, the penetration zone, and in that case the exponent in eq 1 has the value of $n = 2$.

Trying to apply percolation theory to novolak dissolution, one may start by identifying the occupied cells in the percolation field with the OH groups of the phenols. That, however, is not the correct assignment. Base "disappears" whenever it meets a phenol, and in the process the phenol is transformed into a phenolate ion pair.

$$\mathrm{POH} + \mathrm{K^+OH^-} \rightleftarrows \mathrm{PO^-K^+} + \mathrm{H_2O}$$

The phenolate ion pairs so formed are strongly hydrophilic and attract base molecules without reacting with them. *It is the phenolate ion pairs which constitute the hydrophilic percolation sites of the penetration zone.*

0024-9297/92/2225-5345$03.00/0 © 1992 American Chemical Society

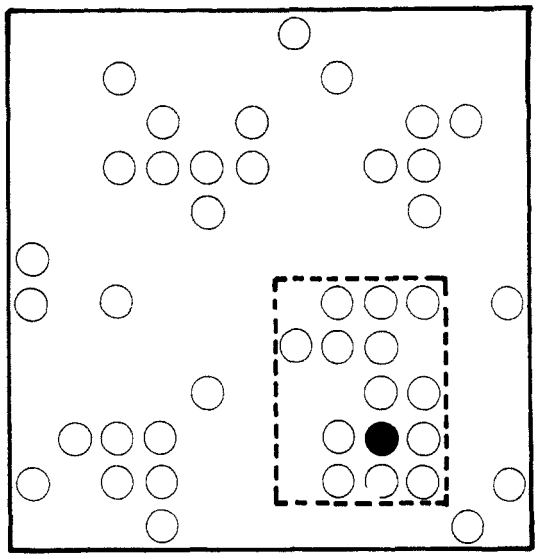

Figure 1. Two-dimensional percolation field.

Modeling the Percolation Field

The main attribute of a percolation site is its attraction for the diffusant. In novolak, which is a medium of low dielectric constant, base is attracted to phenolate or phenol sites principally by electrostatic forces. This interaction can be modeled by a potential energy function of the form[8]

$$V(r) = 4\epsilon\left[\left(\frac{\sigma}{r}\right)^{12} - \left(\frac{\sigma}{r}\right)^{6}\right] - b\mu\left(\frac{\sigma}{r}\right)^{2} + c\left(\frac{\sigma}{r}\right)^{-4} \qquad (2)$$

The first term (in square brackets) is the Lennard-Jones potential between two (nonpolar) particles, characterized by the empirical parameters ϵ and σ, the second term is the Coulombic attraction between an ionic charge and a dipole (μ) oriented in the field of this charge, and the last term models the repulsion experienced by the ion in the hydrophobic environment of the site. The following values of the parameters have been used:

$$\epsilon = 0.018\,75\text{ eV},\quad \sigma = 5\text{ Å},\quad b = 0.1875\text{ eV/D},\quad c = 0.0854\text{ eV}$$

The potential functions calculated from eq 2 for dipole moment values of $\mu = 1.5$ and 3.0 D are plotted in Figure 2. They represent cross sections through (half of) the potential energy wells of the phenol and phenolate percolation sites, respectively.

The process of percolation consists of a succession of transfers of the diffusing base from one hydrophilic site to the next. In making this transition a base molecule must overcome an energy barrier which is defined by the intersection of the potential energy functions of the two neighboring sites (see Figure 3). Assuming that the sites are randomly distributed in the resin, which in *m*-cresol-based novolak and in poly(vinylphenol) derivatives is approximately the case, the average distance between sites (OH groups) is about 5.8 Å. For such a distance and for two identical phenolate sites ($\mu = 3.0$ D), the energy barrier between them is calculated as $E_b = 0.53$ eV. The energy barriers which separate phenolate from phenol sites are somewhat higher, as can be seen in Figure 3. For a phenol site with an effective dipole moment of 1.5 D and for a site separation of 5.8 Å, the energy barrier in Figure 3 is 0.63 eV.

Because of the higher energy barrier, transfer from a phenolate site to a nonionized phenol site is slower than transfer between identical phenolate sites. *Phenolate–phenol transfer which occurs at the front of the penetration zone is, therefore, the rate-determining step in the dissolution process.* The average energy barrier for the phenolate–phenol transition is reflected in the macroscopic activation energy of dissolution. Activation energies of 0.59 eV were measured by Huang et al.[3] for the dissolution of a phenol-based novolak in aqueous KOH. More recently, Shih found an activation energy of 0.62 eV for the dissolution of a poly(vinylphenol) under similar conditions.

The statistical probability of transfer between two sites is determined by a Boltzmann factor, $\exp(-E_b/RT)$, which changes dramatically with the value of the energy barrier E_b. Table I gives the Boltzmann factors for a few values of energy barriers and separations between phenolate sites: the probability of transfer between sites decreases rapidly with increasing site separation.

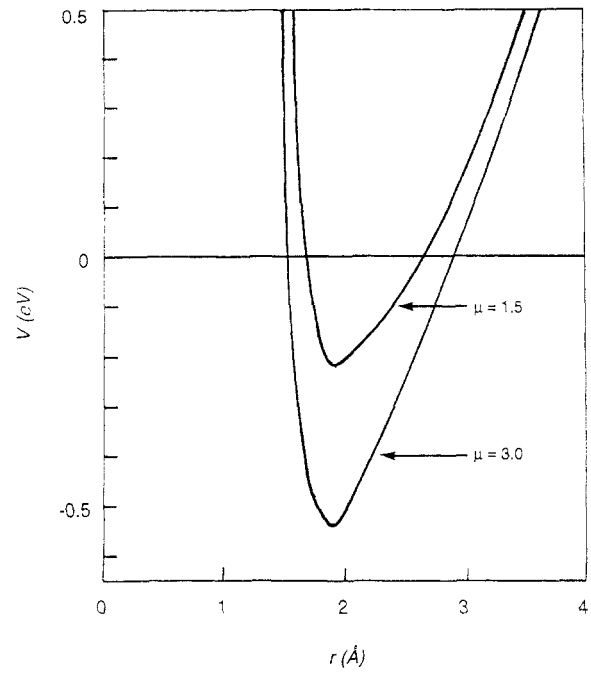

Figure 2. Potential energy functions for the interaction of a monovalent ion with an ion pair (dipole moment μ) in a hydrophobic environment.

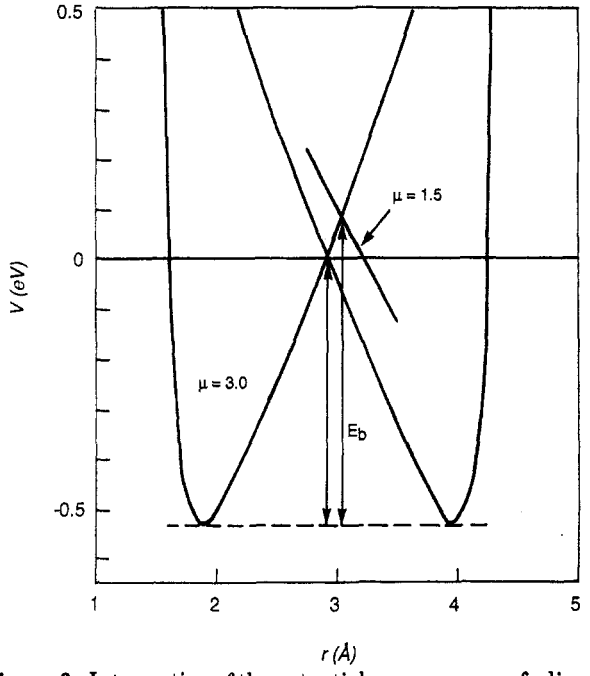

Figure 3. Intersection of the potential energy curves of adjacent sites for a site separation of about 6 Å. The dipole moments of the sites are indicated, as well as the energy barriers E_b.

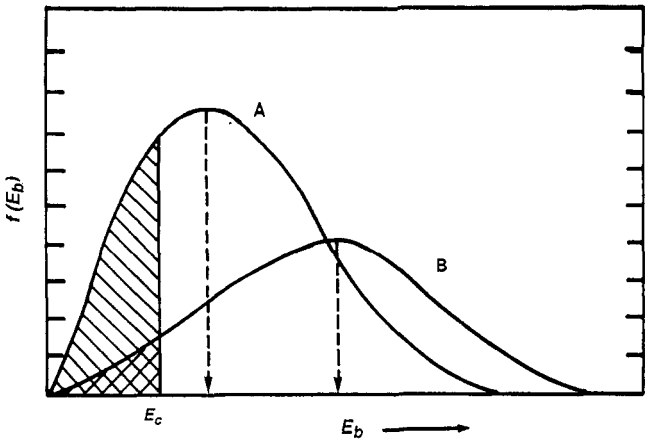

Figure 4. Distribution of energy barriers in an ensemble of sites. The overall site concentration is higher in A than in B.

Table I
Energy Barriers for Transfer of Base between Phenolate Sites

site separation (Å)	energy barrier E_b (kJ/mol)	Boltzmann factor $\exp(-E_b/RT)$
4.0	0.3	8.9×10^{-1}
4.5	2.6	3.5×10^{-1}
5.0	10.6	1.5×10^{-2}
5.5	34.8	9.0×10^{-7}
6.0	60.8	3.1×10^{-11}
6.5	92.7	9.4×10^{-17}

In the ensemble of sites of a phenolic resin there will be a distribution of intersite distances and hence of intersite energy barriers. Two such energy barrier distributions are qualitatively represented in Figure 4. Since intersite energy barriers are of necessity associated with pairs of sites, the distributions in Figure 4 are taken over an ensemble of site pairs. Above a certain critical energy barrier, E_c, the probability of transfer may be deemed negligible, and, furthermore, it will be assumed that transfer is certain for energy barriers smaller than E_c. This crude device allows us to fit the dissolution problem into the established formalism of percolation theory: if E_c has the value indicated in Figure 4, only site pairs contained in the shaded regions under the curves of Figure 4 will take part in the percolation process. (In reality there is no natural discontinuity of transfer probability in these systems. The "critical" energy barrier is a somewhat artificial concept which is, however, needed to make the problem accessible to percolation theory.)

We may replace the term "site pair" by the term "bond" and let the intersite energy barrier decide whether the bond is "open", i.e., passable, or closed. Base migrates then through the solid resin along an unbroken sequence of open bonds, and the penetration zone may be modeled as a bond percolation field. Figure 5 is a cartoon of such a bond percolation field near the percolation threshold.

Several papers have recently dealt with percolative diffusion in three dimensions.[9-13] All assume a uniform array of potentially occupiable percolation cells. The present system differs from those models in that the nature of the sites changes during the diffusion process and that the cells are by no means distributed evenly. The percolation sites in novolak are formed through a chemical reaction of phenolic sites with the diffusant itself, and the resulting percolation network of phenolates is predetermined by the initial distribution of phenol groups in the matrix. As a result the secondary and tertiary structure of the phenolic resin can significantly affect the dissolution process.[14,15]

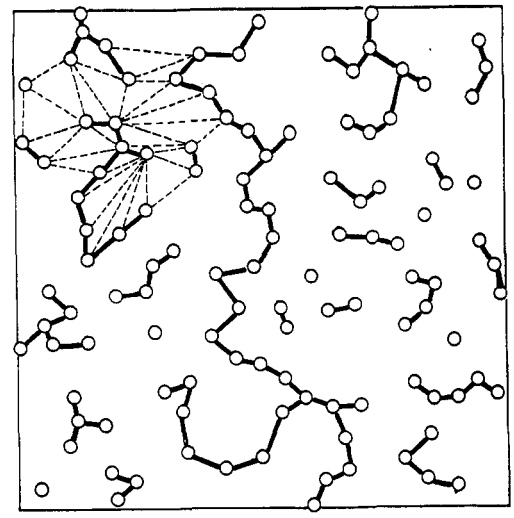

Figure 5. Cartoon of a bond percolation field near the percolation threshold.

Testing the Scaling Law of Percolative Diffusion

In analogy with the theory of ionic conduction in disordered media,[19] percolation theory predicts a relation between the dissolution rate (or diffusion coefficient) and the percolation parameter p in the form of a quadratic law.

$$R = \text{constant} \times (p - p_c)^2 \qquad (3)$$

Equation 3 can be used to test the validity of percolation theory as a model of novolak dissolution.

To carry out such a test, it is necessary to find a way of modulating the percolation parameter p. Since p measures the fraction of occupied percolation cells, it may be assumed that in a phenolic resin p is proportional to the concentration of phenol groups and that it can be modulated by changing the concentration of free phenol moieties in the resin.

Accordingly, we have prepared a range of poly(vinylphenol) resins in which the concentration of free phenol groups was altered by partial methylation. The resins were made from a single brand of poly(vinylphenol) by reacting it with increasing doses of a methylating agent which transformed some of the phenols into nonionizable anisoles. This method of preparation ensured that all resins of the series had the same degree of polymerization.

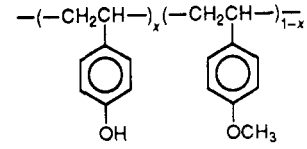

The dissolution rate of the partially methylated resins in aqueous KOH is plotted in Figure 6 as a function of base concentration.

The scaling law of percolative dissolution assumes that the external conditions of the system remain constant and that only its composition changes. The dissolution rate data of the resins to be compared with the predictions of percolation theory were derived from a set of resins where the fraction of free phenol groups was varied in small decrements from 1.00 to 0.72. The relevant rate values were found at the intersection of the dissolution curves with a vertical line of constant c_B (see Figure 7). An aqueous 0.20 N solution of KOH was used as the standard developer.

To derive a value for the percolation parameter p from the composition of the resins, a linear relation between p

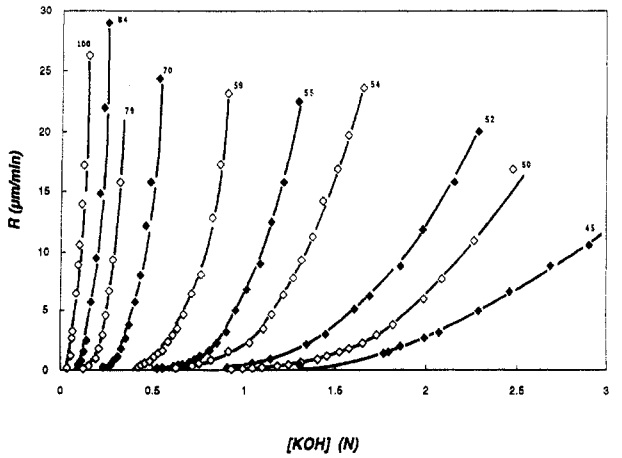

Figure 6. Dependence of the dissolution rate on base concentration in aqueous KOH for a group of partially methylated poly(vinylphenol) resins. The composition of the resins is indicated by the fraction (x) of free phenol groups; R is the dissolution rate in μm/min.

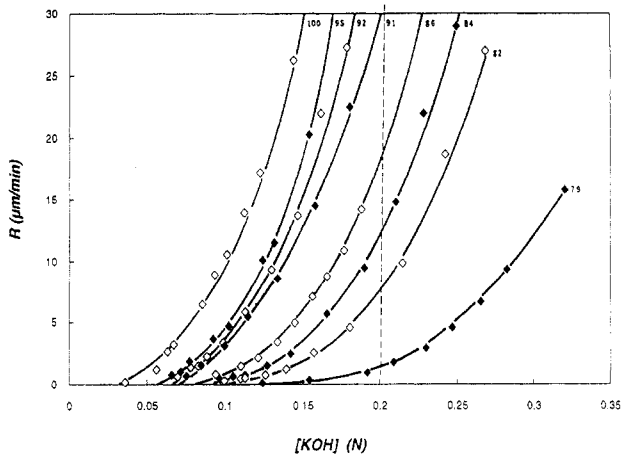

Figure 7. Dependence of the dissolution rate on base concentration in aqueous KOH in a series of partially methylated poly(vinylphenol) resins with fractions of free phenol groups in the range between 1.0 and 0.79.

and the fraction (x) of free phenol groups was assumed.

$$p = ax + b$$

The constants a and b were found from the boundary conditions $p = 1$ for $x = 1$ and $p_c = ax_c + b$. By plotting the experimental values of log R as a function of x, it was found that log R decreased steeply in the vicinity of $x = 0.73$. After some trial and error, a value of $x_c = 0.72$ was adopted for the critical composition threshold. With this and with a percolation threshold of $p_c = 0.20$ for a disordered cubic lattice, the relation between the parameter p and composition x in the series of partially methylated poly(vinylphenol) resins was found to be given by the expression

$$p = 2.86x - 1.86$$

The scaling law of eq 3 was tested in its logarithmic form

$$\log R = \text{constant} + 2 \log (p - p_c) \qquad (4)$$

In Figure 8 a plot of log R against log $(p - p_c)$ derived from the above expression produces a straight line with a slope of 2 as required by theory.

Activation Energy of Dissolution

With the group of partially methylated poly(vinylphenol) resins available, the fundamental assumption of percolative diffusion, namely, that diffusional transport occurs by transfer between discrete sites, can be tested experimentally. If the diffusion process involves sites derived from free phenol groups, dilution of free phenol in the resins is expected to increase the intersite energy barriers, and that should be reflected in the activation energy of dissolution.

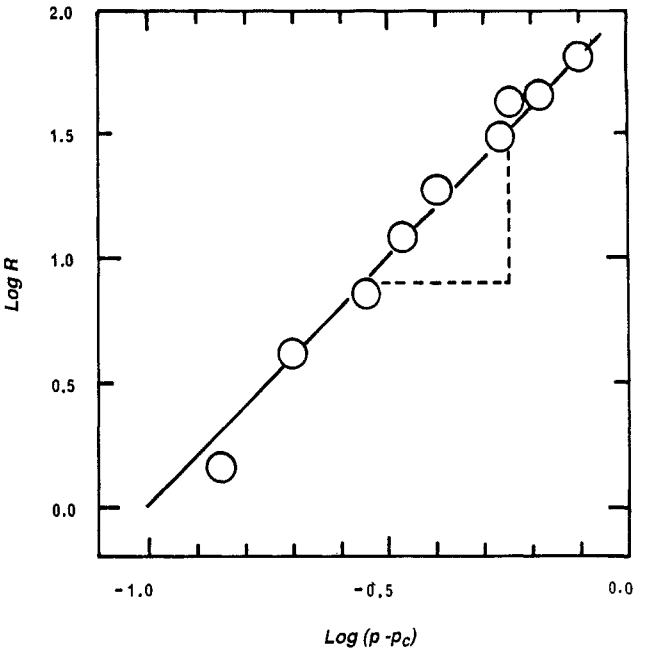

Figure 8. Test of the scaling law of percolative dissolution, eq 4, on a group of partially methylated poly(vinylphenol) resins. R is the dissolution rate (μm/min), p is the percolation parameter, $p = 2.86x - 1.86$, and x is the fraction of free phenol groups in the resin. $p_c = 0.20$ is the percolation threshold in 0.2 N KOH.

Table II
Activation Energies of Dissolution as a Function of the Fraction of Free OH Groups

x	E_a (kJ/mol)	ν (cm^3 × 10^{24})	$\bar{a}$ (Å)
1	38.8	199	5.84
0.95	41.6	211	5.95
0.94	44.7	214	5.98
0.91	45.4	221	6.05
0.86	45.6	236	6.18
0.84	49.9	242	6.23
0.82	52.1	248	6.28
0.77	53.9	266	6.43
0.74	57.8	278	6.52
0.68	65.1	304	6.72
0.63	69.3	330	6.91
0.60	74.5	348	7.03
0.54	79.1	393	7.33
0.52	83.1	405	7.40
0.50	89.5	422	7.50

The activation energy of dissolution was determined for 15 resins with free phenol fractions ranging from 1.00 to 0.50. The data are collected in Table II. Within the range of site densities covered by these experiments the activation energy increases from 38.8 to 89.5 kJ/mol and is an almost linear function of the mean site separation (see Figure 9). This result strongly supports the validity of the percolation model of novolak dissolution.

Dissolution Inhibition

After these preliminaries, a mechanistic insight into the nature of dissolution inhibition comes from the comparison of the dissolution curves $R = f(c_B)$ of a single resin to which increasing quantities of an inhibitor have been added (Figure 10) with the corresponding dissolution curves of a group of partially methylated poly(vinylphenols) in

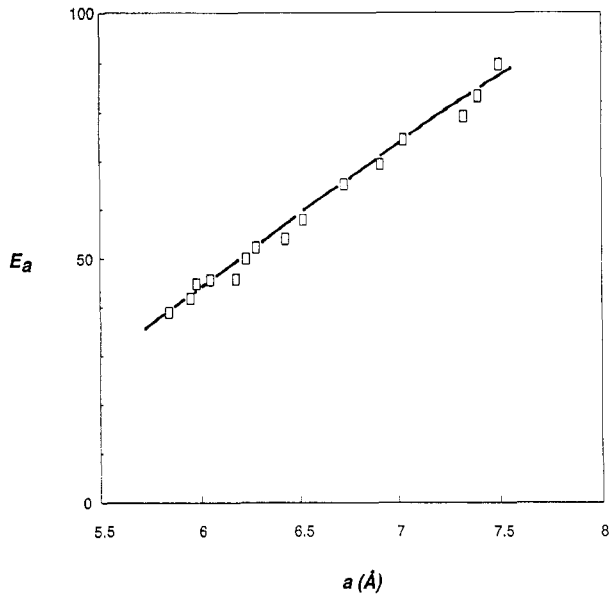

Figure 9. Plot of the activation energies of dissolution in a group of partially methylated poly(vinylphenols) as a function of the average intersite distance a.

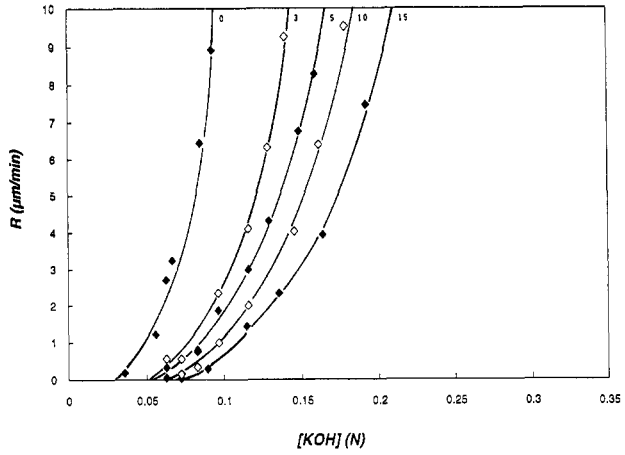

Figure 10. Dependence of the dissolution rate on base concentration for a poly(vinylphenol) resin (MW 22 000) doped with increasing quantities of our standard inhibitor. The inhibitor content is noted on the curves.

Figure 7. The similarity between the two representations suggests that the addition of an inhibitor to the phenolic resin is tantamount to a reduction in the number of hydrophilic sites. Recent experimental work[16-19] indicates a strong interaction between inhibitors and free phenol groups. In light of these results it may be said that the system in Figure 10 behaves as if the inhibitor was blocking some of the phenols and shielding them from the approach of developer base. The equivalency of inhibition to a lowering of the concentration of hydrophilic sites implies a relation between inhibition and the percolation parameter p. Before this idea can be further explored it is necessary to introduce a quantitative measure of dissolution inhibition.

Meyerhofer[20] has shown that the logarithm of the dissolution rate, R_i, of an inhibited resin is usually a linear function of the concentration, c_i, of inhibitor. In Figure 11 $\log R_i/R_0$ is plotted as a function of c_i and can be seen to have a constant slope over a useful range of inhibitor concentration. This slope will be termed the inhibition factor, f_{ij}, of inhibitor i in resin j,[21] and it will be used as

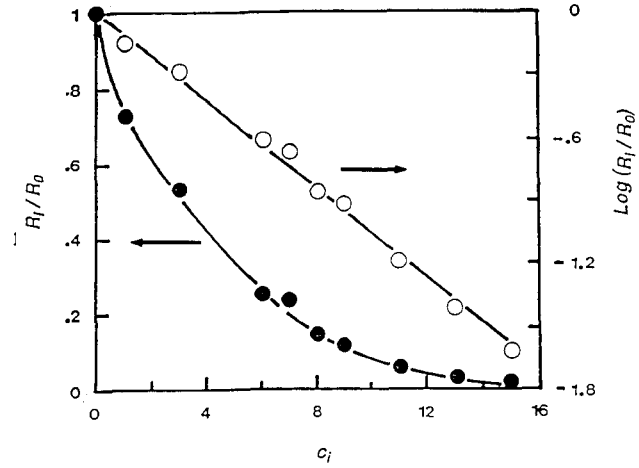

Figure 11. Plot of the ratio of the dissolution rate R_i of the inhibited resin to the dissolution rate R_0 of the pure resin and the logarithm of this ratio as a function of the inhibitor content, c_i (weight percent), in the resin.

a concentration-independent measure of the inhibition capacity of the additive.

$$-\frac{\mathrm{d}\log(R_i/R_0)}{\mathrm{d}c_i} = f_{ij} \tag{5}$$

Inhibition as well as the reduction in the number of hydrophilic sites corresponds to a lowering of the percolation parameter p; the relation between the inhibition factor f_{ij} and the dissolution rate can, therefore, be expressed in the following form.

$$-\frac{\mathrm{d}\log R}{\mathrm{d}c_i} = f_{ij} = \text{constant} \times \frac{\mathrm{d}\log R}{\mathrm{d}p} \tag{6}$$

To visualize the meaning of eq 6, a plot of $\log R$ against the percolation parameter p is shown in Figure 12. The derivative $\mathrm{d}\log R/\mathrm{d}p$ represents the tangent to this function at any image point ($\log R$,p). The addition of a certain quantity of inhibitor translates the image point of the resin by a fixed horizontal distance toward lower values of p. It can be seen that this effect will be significantly more important in slowly dissolving resins, with image points nearer the percolation threshold, than in fast dissolving resins near $p = 1$.

This link between inhibition and dissolution rate had been discovered empirically by resist designers[16] a long time ago; the percolation model provides now a simple intuitive interpretation. Base diffusion occurs by successive transfers within a network of hydrophilic sites, the elimination of some of these stepping stones by the inhibitor will have its greatest effect near the critical state of the percolation field where the diffusional flux is conducted through a small number of infinite percolation clusters and possibly through a single such cluster. Under these conditions, the removal of a few crucial connections can interrupt the diffusional flow almost completely, while in a dense percolation field the disappearance of a few hydrophilic sites will not make much of a difference.

Equation 6 can be rewritten in the form

$$f_{ij} = \alpha_i \frac{2\log e}{p - p_c} \tag{7}$$

which relates the inhibition factor of an additive directly to the percolation parameter or rather to the difference $(p - p_c)$. It can be seen that, as the percolation parameter of the resin approaches the percolation threshold p_c, the inhibition factor increases and tends toward infinity.

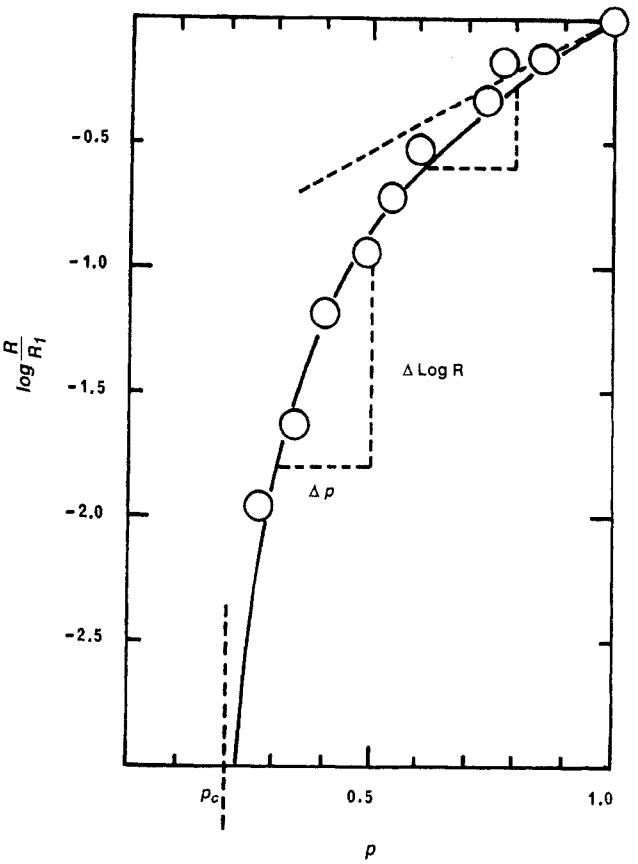

Figure 12. Dimensionless presentation of the dependence of the logarithm of the dissolution rate on the percolation parameter p. R_1 is the dissolution rate of the system at $p = 1$. The experimental points refer to the series of partially methylated poly(vinylphenols) described in the text.

Equation 7 was tested quantitatively on the series of partially methylated poly(vinylphenols). The inhibition factor for the generic inhibitor, the 4-*tert*-butylphenyl ester of 2,1-naphthodiazoquinone-5-sulfonic acid, was determined in nine different resins. The resists were all developed in 0.2 N KOH. The percolation parameter p was again derived from the composition of the resins (x) via the expression $p = 2.86x - 1.86$, and the percolation threshold was taken as $p_c = 0.20$. In Figure 13 the inhibition factors of the resins are plotted against the corresponding values of $d \log R/d_p = 0.8686/(p - p_c)$. The plot is linear, in agreement with the basis assumptions of the percolation model.

This treatment of inhibition has an interesting corollary. The slope of the plot in Figure 13 defines a constant (α_i) which measures the inherent inhibition capability of the inhibitor without reference to any particular resin. Within the validity of eq 7 this parameter allows an objective comparison of different inhibitors and assigns a general and "absolute" figure of merit to any additive. The inhibition factor f_{ij} of an additive i in resin j is generated from α_i by multiplication with the factor

$$0.8686/(p - p_c)$$

where p is the value of the percolation parameter of resin j.

Insensitivity of Inhibition to the Size of the Base Cation

As a last test for the validity of the percolation model of dissolution inhibition, the effect of the size of the cation of the developer base on the inhibition effect was investigated. The dissolution rate of a single resin doped with

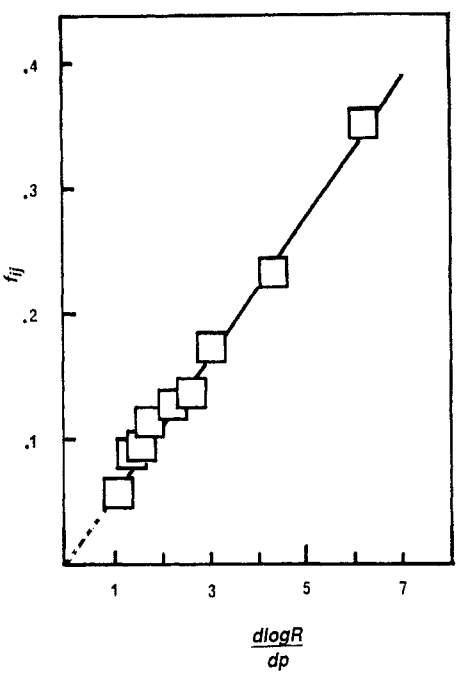

Figure 13. Experimental test of the interrelation between inhibition and dissolution rate, eq 6. The inhibition factor f_{ij} is plotted against the slope of the dimensionless master curve in Figure 12.

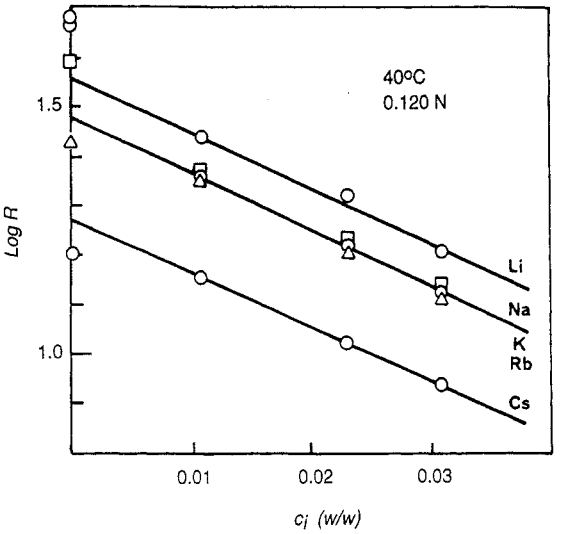

Figure 14. Plot of the logarithm of the dissolution rate of a single resin doped with increasing quantities of the standard inhibitor and developed in 0.2 N solutions of the alkali hydroxides LiOH, NaOH, KOH, RbOH, and CsOH.

increasing quantities of our standard inhibitor was measured in 0.2 N solutions of different alkali hydroxides. In going from LiOH to CsOH the dissolution rates changed substantially, but the slope of a plot of log R vs c_i, which defines the inhibition factor, remained the same (Figure 14).

This result agrees with the intuitive concept of percolative diffusion: The inhibitor modifies the percolation field in a way that can be likened to the setting up of an obstacle course. The obstacles interfere with the progress of the diffusant, but the factor by which the diffusant is slowed down in the system is the same for fast-diffusing particles as for slowly diffusing ones.

Discussion

The model presented in this study contains many approximations. The most blatant simplification of the model is the introduction of a critical intersite energy

barrier which distinguishes between open and closed bonds in a discontinuous way. This assumption makes it possible to fit the phenomenon of resin dissolution into the conventional modes of percolation theory, but we believe that very careful experimentation near the percolation threshold would show that the continuous distribution of intersite barriers leads to a blurring of the line between open and closed bonds and makes the threshold less definite. A similar effect is brought about by the finite thickness of the penetration zone, which the model treats as an infinite percolation field. Some of these concerns are addressed in Chapter 4 of ref 7.

Also the description of the potential energy functions of the hydrophilic sites by eq 2 is not quite accurate; the numerical agreement between the average intersite energy barrier of unmethylated poly(vinylphenol) and the experimentally determined activation energy of dissolution is the result of the choice of the empirical parameters. The shortcomings of the representation show up in the dependence of the activation energy on the average site separation plotted in Figure 9. This dependence is somewhat steeper than the prediction based on the potential energy curves shown in Figure 3. However, the main point of the argument is that the activation energy does depend on the concentration of phenols in the materials, which proves that discrete sites are involved in the diffusion process. The specifics of the electrostatic model do not enter into percolation theory; it is enough that the hydrophilic sites attract the diffusant to ensure the applicability of a percolation approach. Percolation theory manages to perform so well here also because scaling laws are notoriously forgiving. The reader is referred to the work of de Gennes[22] and his collaborators where exceedingly complex microscopic behavior leads to surprisingly simple macroscopic relations.

The percolation model as it is presented here has the merit of promoting an intuitive grasp of the mechanism of dissolution and dissolution inhibition. Within the limits of the model's validity the qualitative features of the dissolution kinetics of all phenolic resins flow from a single mental picture, the percolation field. The contribution of percolation theory to the understanding of the system is the realization that the state of the field is determined entirely by the value of the percolation parameter p which characterizes the resin. In a phenolic resin the percolation parameter is linked to the concentration of hydrophilic phenol sites and to the prevailing distribution of intersite energy barriers. The rate of dissolution is determined by the number of continuous, uninterrupted diffusional pathways through the penetration zone, and that is related to the number of infinite clusters of hydrophilic sites. The qualitative behavior of most resists can be envisioned on the basis of these concepts.

The quadratic form of the scaling law has significant consequences for the photographic performance of resists based on dissolution inhibition. The logarithm of the dissolution rate decreases precipitously as p approaches the percolation threshold, and the function $\log R = f(p)$ approaches infinity with an infinite negative slope. However, the dissolution rate itself has its origin at $R = 0$, $p = p_c$, and starts out from there with an initial slope of zero (see Figure 15). This is to be contrasted with the behavior of cross-linking systems. Gel formation via cross-links can again be represented by a percolation model, but here the gelation process takes place by percolative cross-linking in a Bethe lattice[7] of quasi-infinite dimensionality, and the exponent of the scaling law is 0.4. The strength, P, of the cross-linked network is plotted in Figure 15 as a function of the percolation parameter (the cross-link density) and can be seen to rise from the origin at p_c, the gel point, with an infinite positive slope. At the gel point, gel formation corresponds thus to a secondary phase transition, while the dissolution of novolak does not. That is the fundamental reason why radiation-sensitive cross-linking systems have higher photographic speed (are more sensitive) than the traditional positive photoresists.

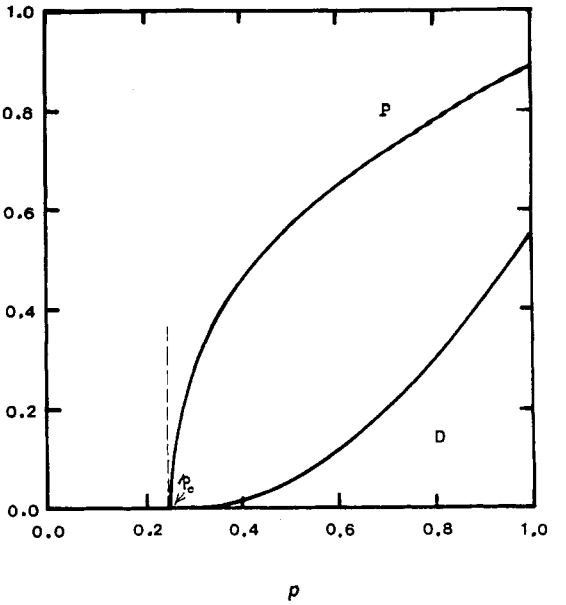

Figure 15. Plot of the network strength P and the diffusion coefficient D as a function of the percolation parameter p. The percolation threshold is assumed to be $p_c = 0.25$.

An illuminating discussion of the explosionlike percolative growth of cross-linked networks can be found in Flory's book.[23]

Percolation theory points the way to the optimization of the phenolic resin used as a resist. Base diffuses in the percolation field through a network of open bonds; the smaller the number of possible pathways leading across the field (the penetration zone), the easier it will be to interrupt the diffusion process and inhibit dissolution. The image point of the resin to be used for the resist should, therefore, be as near as possible to the percolation threshold on the master curve of Figure 12. Practical considerations, e.g., the necessity of an acceptable rate of development, will place a limit on the attainment of ultimate sensitivity, but the direction in which the design of the material should proceed is now clearly understood. The criteria by which the structure of inhibitors may be optimized will be considered in another paper.

Experimental Part

Materials. A group of partially methylated poly(vinylphenol) resins was prepared as follows. A single brand of poly(vinylphenol) (MW 22 000) was obtained from Polysciences. The polymer was purified by refluxing a methanolic solution containing hydrochloric acid for 3 h and precipitating the polymer into water. Samples of this material were treated with increasing quantities of dimethyl sulfate. For example, 8.0 g of purified poly(vinylphenol) (0.73 mol of OH) was dissolved in 150 mL of a 10% aqueous solution of KOH to which 3.0 mL of dimethyl sulfate (0.032 mol) was added. After refluxing this solution under nitrogen for 1 h, the polymer was precipitated into acidic water. The crude product was purified by dissolution in acetone and reprecipitation into water, and this procedure was repeated twice. The final product was dried at 90 °C (3 mmHg) for 8 h. The yield was 70% based on methylated phenol groups.

The partially methylated resins were characterized by NMR. The contents of free phenol groups was estimated from proton

NMR spectra taken in acetone-d_6 solution on a Varian EM390 NMR spectrometer. The integrated signal of the OH protons was calibrated on the internal standard of the protons of the benzene ring. The result was checked by elemental analysis performed by Quantitative Technologies, Inc.

Determination of the Dissolution Rate. The resins were spin-coated from 25–28% solutions in isoamyl acetate onto 2-in. silicone wafers. The coated wafers were prebaked in a vacuum oven for 1 h at 90 °C. The samples were then placed in a beaker with a known aqueous solution of KOH. The concentration of KOH in the developer was checked by titration before every run. The change of film thickness during development was monitored by laser interferometry as described in ref 21. The dissolution rate was derived from the reflection data by the method of Rodriguez et al.[24]

The inhibition effect of the generic inhibitor, the 4-*tert*-butylphenyl ester of 2,1-naphthodiazoquinone-5-sulfonic acid, was measured by mixing the base resin with increasing quantities of this inhibitor (2–10% by weight), coating the resist on silicone wafers as before, and determining the dissolution rate in 0.2 N aqueous KOH.

Acknowledgment. We are grateful to the Office of Naval Research and to the National Science Foundation for financial support of this work. We also thank Professor Alla Margolina of Polytechnic University and Dr. Ralph Dammel of Hoechst Celanese Corp. for helpful discussions.

References and Notes

(1) Suess, O. *Annalen* **1944**, *556*, 65.
(2) Kalle AG. German Patent 879,204, 1949.
(3) Huang, J. P.; Kwei, T. K.; Reiser, A. *Macromolecules* **1989**, *22*, 4106.
(4) Huang, J. P.; Pearce, E. M.; Reiser, A.; Kwei, T. K. *Polymers in Microelectronics*; ACS Symposium Series 412; American Chemical Society: Washington, DC, 1989; p 364.
(5) Arcus, R. A. *Proc. SPIE* **1986**, *631*, 124.
(6) Essam, J. W. Percolation Theory. *Rep. Prog. Phys.* **1980**, *43*, 833–912.
(7) Stauffer, D. *Introduction to Percolation Theory*; Taylor and Francis: London, 1985.
(8) Berry, R. S.; Rice, S. A.; Ross, J. *Physical Chemistry*; John Wiley: New York, 1980; pp 417–419.
(9) Sapoval, B.; Rosso, M.; Gouyet, J. F. *J. Phys. Lett.* **1985**, *46*, L-149.
(10) Rosso, M.; Gouyet, J. F.; Sapoval, B. *Phys. Rev. Lett.* **1986**, *57*, 3195.
(11) Trefonas, P. *Proc. SPIE* **1986**, *1086*, 484.
(12) Bogdanov, A. L.; Valiev, K. A.; Velikov, L. V.; Zaroslav, D. Y. *J. Vac. Sci. Technol.* **1987**, *5*, 391.
(13) Silverman, B. D. *Macromolecules* **1991**, *24*, 2467.
(14) Roeschert, H.; Gordon, D. J.; Hinsberg, W. D.; McKean, D.; Lindley, C. R.; Merrem, H. J.; Pawlowski, G.; Sauer, T.; Vicari, R.; Willson, C. G.; Dammel, R. *Proc. SPIE* **1990**, *1262*, 391.
(15) Hanabata, M.; Uetani, Y.; Furuta, A. *J. Vac. Sci. Technol.* **1989**, *B7*, 640.
(16) Koshiba, M.; Murata, M.; Matsui, M.; Harita, Y. *Proc. SPIE* **1988**, *920*, 364.
(17) Murata, M.; Koshiba, M.; Harita, Y. *Proc. SPIE* **1989**, *1086*, 48.
(18) Honda, K.; Beauchemin, B. T.; Hurditch, R. J.; Blakeney, A. J.; Kawabe, Y.; Kokubo, T. *Proc. SPIE* **1990**, *1262*, 493.
(19) Honda, K.; Beauchemin, B. T.; Fitzgerald, E. A.; Jeffries, A. T.; Tadros, S. P.; Blakeney, A. J.; Hurditch, R. J.; Tan, S.; Sagakuchi, S. *Proc. SPIE* **1991**, *1466*, 141.
(20) Meyerhofer, D. *IEEE Trans. Electron Devices* **1980**, *ED-27*, 921.
(21) Yeh, T.-F.; Shih, H.-Y.; Reiser, A.; Toukhy, M. A.; Beauchemin, B. T., Jr., submitted for publication in *J. Vac. Sci. Technol.*
(22) de Gennes, P.-G. *Scaling Concepts in Polymer Physics*; Cornell University Press: Ithaca, NY, and London, 1979.
(23) Flory, J. P. *Principles of Polymer Chemistry*; Cornell University Press: Ithaca, NY, 1953; p 348ff.
(24) Rodriguez, F.; Krasicky, P. D.; Groele, R. J. *Solid State Technol.* **1985**, *28* (5), 125.

Registry No. Poly(vinylphenol), 59269-51-1.